Phase Behavior of the Mixtures of CO_2 + Poly(methyl methacrylate) + Ethanol at High Pressure

Kiyoshi Matsuyama* and Kenji Mishima

Department of Chemical Engineering, Fukuoka University 8-19-1 Nanakua, Jonan-ku, Fukuoka 814-0180, Japan

Phase equilibria of carbon dioxide (CO_2) + poly(methyl methacrylate) (PMMA-15 k, PMMA-120 k) + ethanol ternary systems were measured at temperatures ranging from (293.3 to 359.7) K and pressures up to 14.1 MPa. Furthermore, cloud point temperatures of PMMA + ethanol binary systems were determined at pressures up to 15 MPa. To determine the phase boundary, we observed the cloud points and bubble points by using a variable volume view cell. With the addition of CO_2 into the binary PMMA + ethanol mixture, the upper critical solution temperature (UCST) line shifts toward higher pressure and temperature values. At high CO_2 concentrations, the lower critical solution temperature (LCST) and UCST curves merge. Further, the liquid–liquid split phenomenon is observed over the entire temperature range.

Introduction

CO_2-expanded liquids are a novel class of sustainable solvents because they offer several advantages over both the conventional organic solvents and supercritical CO_2. CO_2-expanded liquids exhibit lower viscosity and higher diffusion coefficients than the conventional organic solvents. As the result of these advantages, CO_2-expanded liquids can be applied in several processes such as nanoparticle formation, homogeneous reactions, catalytic reactions, and polymeric materials formation.[1–5] Furthermore, CO_2-expanded liquids are advantageous for polymer processing[6–9] because many polymers dissolve in CO_2-expanded liquids as compared to supercritical CO_2 with a small amount of cosolvent. In previous studies, we demonstrated the use of the pressure-induced phase separation (PIPS) of CO_2-expanded ethanol in obtaining polymeric microparticles and polymer composite particles.[9] In these particle formation techniques, CO_2-expanded ethanol is generally selected as the solvent since it is an environmentally benign solvent. CO_2 is nonflammable, inexpensive, and particularly nontoxic. Moreover, ethanol is more environmentally acceptable than many organic solvents. To design and optimize these processes, it is important to understand the phase behavior of CO_2-expanded liquids because the product morphology is strongly affected by the phase behavior. However, polymer solutions containing CO_2 exhibit extremely complex phase equilibrium behavior because the large differences among the physical properties of the polymer, solvent, and CO_2 induce complicated physicochemical interactions in polymer solutions containing CO_2.[10] Thus, many researchers have reported the phase behavior of polymer solutions containing CO_2.[10–16] To develop an effective method for the production of polymeric materials by using CO_2-based technology that employs CO_2-expanded liquids and/or supercritical CO_2 with cosolvents, it is essential to understand the phase behavior of CO_2 + polymer + cosolvent systems under elevated pressures and temperatures.

In this study, the phase equilibria of the poly(methyl methacrylate) (PMMA-15 k, PMMA-120 k) + ethanol and CO_2 + PMMA + ethanol systems are determined. The effects of pressure, temperature, and molecular weight of PMMA on the phase equilibria are discussed.

* Corresponding author. Fax: +81(92)865-6031. Phone: +81(92)871-6631. E-mail: mtym@fukuoka-u.ac.jp.

Experiment

Materials. Carbon dioxide (CO_2) with a minimum purity of 99.9 % was purchased from Fukuoka Sanso Co., Ltd. Ethanol with purities greater than 99.5 % was obtained from Wako Pure Chemical Industry Co., Ltd. The poly(methly methacrylate) (PMMA) samples—PMMA-15 k (M.W. = 15 000) and PMMA-120 k (M.W. = 120 000)—were purchased from Aldrich Co.

Apparatus and Procedure. The details of the variable volume view cell used in the procedures for the measurement of the cloud point of the polymer solution containing CO_2 are described in our previous paper.[16] The experimental apparatus included a variable volume view cell, hand pump, and heater jacket. The internal volume of the cell could be varied from (10 to 150) cm^3 by moving a free piston with a distance of 50 mm along the cell. A Teflon-coated magnetic stirring bar was used to ensure thermal and phase equilibria. The phase transition was observed through a quartz glass window, and the images were captured with an optical unit (CCD camera) and displayed on a monitor. The cell was surrounded by the heater jacket at the desired temperature, which was controlled to within 0.1 K. The temperature of the sample in the cell was measured with a platinum resistance thermometer. The uncertainty in the temperature measurement was 0.1 K. The pressure was supplied by using a hand pump and measured with a digital gauge. The uncertainty in the measured pressure was estimated to be 0.2 MPa.

Known amounts of ethanol and PMMA (in the form of particles) were loaded directly into the cell. To remove the air, CO_2 was circulated in the cell at atmospheric pressure. The solution in the cell was compressed by moving the piston inside the cell by using the hand pump and agitated by using the magnetic bar until it became a single-phase solution. The cell was then heated to the desired temperature. After the solution was observed to maintain a single phase, it was charged with CO_2. The system pressure was controlled by moving the piston. The uncertainty in the amounts of PMMA and ethanol was

10.1021/je7007473 CCC: $40.75
Published on Web 04/10/2008

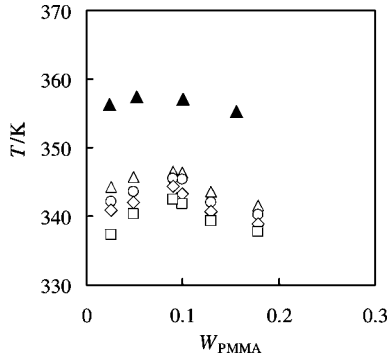

Figure 1. Cloud point temperature of the PMMA + ethanol systems for pressures ranging from the vapor pressure of ethanol solution containing PMMA to 15 MPa: Δ, PMMA-15 k at vapor pressure; ○, PMMA-15 k at 5 MPa; ◇, PMMA-15 k at 10 MPa; □, PMMA-15 k at 15 MPa; ▲, PMMA-120 k at vapor pressure.

estimated to be ± 0.02 g. After the cloud point measurement, the actual weight of CO_2 was determined by using a wet gas meter. A cold trap containing ethanol was used before using the wet gas meter to collect the ethanol and PMMA. To determine the CO_2 remaining in the cell after decompression to atmospheric pressure, it was purged by moving the piston. The uncertainty in the amount of CO_2 was estimated to be ± 0.5 g.

In this study, three types of phase behavior were observed. These were exhibited as the L−LV coexistence curves, L−LL coexistence curves, and LL−LLV coexistence curves. The L−LV coexistence curves indicate the liquid → liquid + vapor transition points, and the L−LL coexistence curves indicate the liquid → $liquid_1$ + $liquid_2$ transition points. These phase-transition points were visually observed by lowering the pressure at the isotherm. The L−LL curve actually represents the upper critical solution temperature (UCST) curve that is the cloud point curve. We defined the cloud point as the composition at which the magnetic bar could no longer be observed visually.[17] After the cloud point was measured, the pressure was reduced further to measure the phase transition boundary of the LL−LLV curve. The LL−LLV coexistence curves indicate the $liquid_1$ + $liquid_2$ → $liquid_1$ + $liquid_2$ + vapor transition points. To investigate the L−LV curves and the LL−LLV curves, the pressure of the single-liquid phase in the cell was decreased to a constant temperature until the first bubble of the vapor appeared visually.[17]

Results and Discussion

PMMA + Ethanol Binary Systems. Figure 1 and Table 1 show the variation in the cloud point temperature of a PMMA + ethanol system by means of a temperature−composition phase diagram under pressures ranging from the solvent-saturated vapor pressure to 15 MPa. Under our experimental conditions, the UCST behavior is observed. A similar phase behavior was exhibited by the PMMA + cyclohexanol system.[18] Under the ethanol-saturated vapor pressure conditions, the cloud point temperature of the PMMA-120 k + ethanol system is higher than that of the PMMA-15 k + ethanol system. It is well-known that polymers with high molecular weights exhibit considerably low solubilities as compared to those with low molecular weights.[19]

Furthermore, we discuss the effect of pressure on the cloud point temperatures of the PMMA-15 k + ethanol system. The UCST demixing is slightly influenced by pressure. For example, the cloud point temperatures around the UCST were found to vary by only 5 K for a change in concentration (weight fraction) from 0.0257 to 0.179 under pressures ranging from the solvent-saturated vapor pressure to 15 MPa. The UCST demixing is slightly influenced by pressure.[15,17]

Table 1. Cloud Point Temperatures of the PMMA + Ethanol Binary Systems under Pressures Ranging from the Vapor Pressure to 15 MPa

weight fraction of PMMA(−)	cloud point temperature (K)
PMMA-120 k	
P = Vapor Pressure	
0.0244	356.3
0.0520	357.5
0.100	357.1
0.156	355.3
PMMA-15 k	
P = Vapor Pressure	
0.0257	344.3
0.0492	345.8
0.0903	346.6
0.100	346.5
0.129	343.7
0.179	341.6
P = 5 MPa	
0.0257	342.2
0.0492	343.7
0.0903	345.6
0.0995	345.4
0.129	342.1
0.179	340.3
P = 10 MPa	
0.0257	340.9
0.0492	342.1
0.0903	344.4
0.0995	343.3
0.129	340.7
0.179	338.9
P = 15 MPa	
0.0257	337.3
0.0492	340.4
0.0903	342.5
0.0995	341.8
0.179	337.8
0.129	339.4

CO_2 + PMMA-15 k + Ethanol Ternary System. For the CO_2 + PMMA-15 k + ethanol ternary system, the measured phase transition pressure at various concentrations of CO_2 is summarized in Figure 2 and Table 2. The concentration of PMMA-15 k in ethanol (CO_2-free) was fixed as 5 wt % in this system.

When CO_2 up to 11.4 wt % was added to the PMMA-15 k + ethanol solutions, PMMA-15 k was completely dissolved in the CO_2-expanded liquid (ethanol) phase at temperatures ranging from (293.3 to 359.7) K. As shown in Figure 2(a), only L−LV coexistence points were observed at low concentrations of CO_2. The L−LV curve denotes the phase-transition points (bubble point) of the polymer solution from a single-liquid phase to L + V phases. On the other hand, the solid PMMA-15 k phase was observed at 0 wt % CO_2 under our experimental conditions.

Furthermore, when CO_2 up to 41.4 wt % was added, the UCST curve appeared as shown in Figure 2(b). The UCST curve represents the phase transition points (cloud point) from a single-liquid phase to the L + L phases under reduced pressure. In the present study, it was not possible to accurately measure the upper critical end point (UCEP) and lower critical end point (LCEP) values at which the LV, LLV, and LL loci converge. However, the existence of a UCEP can be predicted in the region where the L−LV and UCST curves coexist. The UCEP shifted

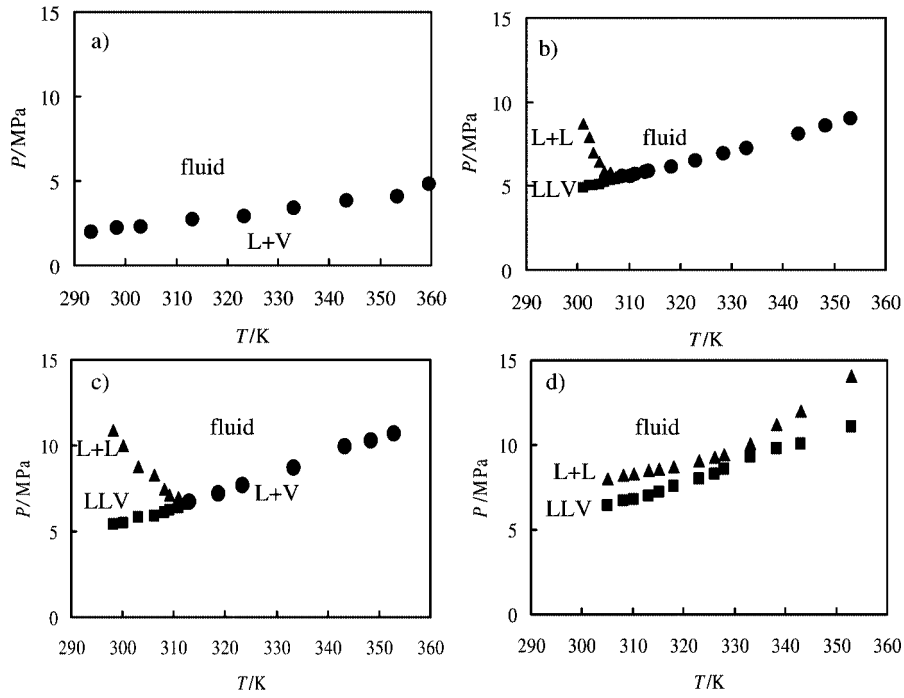

Figure 2. Pressure and temperature phase diagrams for the CO_2 + PMMA-15 k + ethanol system. (a) 11.4 wt % CO_2 + 4.5 wt % PMMA + 84.1 wt % ethanol. (b) 41.4 wt % CO_2 + 2.9 wt % PMMA + 55.7 wt % ethanol. (c) 51.2 wt % CO_2 + 2.5 wt % PMMA + 46.3 wt % ethanol. (d) 56.9 wt % CO_2 + 2.2 wt % PMMA + 40.9 wt % ethanol. Symbols: ●, liquid → liquid + vapor (LV) transition point (bubble point); ▲, liquid → liquid$_1$ + liquid$_2$ (LL) transition points (cloud point); ■, liquid$_1$ + liquid$_2$ → liquid$_1$ + liquid$_2$ + vapor (LLV) transition points.

Table 2. Experimental Cloud Point and Bubble Point Data for the CO_2 + PMMA-15 k + Ethanol System

T (K)	P (MPa)	transition	T (K)	P (MPa)	transition	T (K)	P (MPa)	transition	T (K)	P (MPa)	transition
11.4 wt % CO_2 + 4.5 wt % PMMA + 84.1 wt % ethanol			41.4 wt % CO_2 + 2.9 wt % PMMA + 55.7 wt % ethanol			51.2 wt % CO_2 + 2.5 wt % PMMA + 46.3 wt % ethanol			56.9 wt % CO_2 + 2.2 wt % PMMA + 40.9 wt % ethanol		
293.3	2.0	VL	308.7	5.6	VL	313.2	6.7	VL	305.2	8.0	LL
298.4	2.2	VL	310.4	5.6	VL	318.7	7.2	VL	308.3	8.2	LL
303.2	2.3	VL	311.4	5.7	VL	323.4	7.7	VL	310.2	8.3	LL
313.2	2.7	VL	313.3	5.8	VL	333.4	8.7	VL	313.2	8.5	LL
323.4	2.9	VL	313.8	5.9	VL	343.5	9.9	VL	315.2	8.6	LL
333.2	3.4	VL	318.4	6.1	VL	348.5	10.3	VL	318.2	8.7	LL
343.4	3.8	VL	323.0	6.5	VL	353.0	10.7	VL	323.0	9.1	LL
353.5	4.1	VL	328.5	6.9	VL	298.2	10.9	LL	326.2	9.3	LL
359.7	4.8	VL	333.0	7.2	VL	300.3	10.0	LL	328.0	9.4	LL
			343.0	8.1	VL	303.2	8.8	LL	333.3	10.1	LL
			348.3	8.6	VL	306.2	8.3	LL	338.4	11.2	LL
			353.2	9.0	VL	308.2	7.5	LL	343.2	12.0	LL
			301.2	8.7	LL	309.2	7.1	LL	353.1	14.1	LL
			302.3	7.9	LL	310.9	7.0	LL	305.2	6.4	VLL
			303.2	7.0	LL	312.3	6.7	LL	308.3	6.7	VLL
			304.2	6.4	LL	298.2	5.4	VLL	310.2	6.8	VLL
			305.2	5.9	LL	300.3	5.5	VLL	313.2	7.0	VLL
			306.4	5.8	LL	303.2	5.8	VLL	315.2	7.2	VLL
			307.4	5.5	LL	306.2	5.9	VLL	318.2	7.6	VLL
			301.2	4.9	VLL	308.2	6.1	VLL	323.0	8.0	VLL
			302.3	5.0	VLL	309.2	6.2	VLL	326.2	8.3	VLL
			303.2	5.0	VLL	310.9	6.4	VLL	328.0	8.6	VLL
			304.2	5.1	VLL	312.3	6.6	VLL	333.3	9.3	VLL
			305.2	5.2	VLL				338.4	9.8	VLL
			306.4	5.3	VLL				343.2	10.1	VLL
			307.4	5.4	VLL				353.1	11.1	VLL

to higher temperature regions from (305 to 312) K, as shown in Figure 2(c). Also, the phase transition pressure increased significantly with the amount of CO_2 added to the system. When the CO_2 concentration is increased to 56.9 wt %, we can obtain a $P-T$ diagram to show the dramatic disappearance of the UCST curves, as illustrated in Figure 2(d). It may be considered that the UCST and lower critical solution temperature (LCST) curves merge with an increase in the CO_2 concentration. Although the LCST curve was not observed in our experimental conditions, the LCST appeared at CO_2 concentrations ranging from (51.2 to 56.9) wt %. In the CO_2 + PMMA-15 k + ethanol system, it can be stated that the pressure conditions in which the liquid–liquid split phenomenon was observed are present over the entire temperature range in which the CO_2 concentration was greater than 59.9 wt %.

Finally, the effects of the composition and molecular weight of the PMMA on the liquid–liquid (LL) phase boundary of the CO_2 + PMMA + ethanol systems were investigated. The cloud

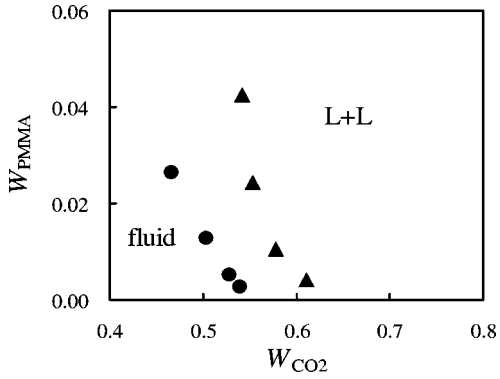

Figure 3. Cloud point compositions (weight fraction) for the CO_2 + PMMA + ethanol + system at 15 MPa and 373.2 K: ▲, PMMA-15 k; ●, PMMA-120 k.

Table 3. Cloud Point Compositions (Weight Fraction) of the CO_2 (1) + PMMA (2) + Ethanol (3) System at 15 MPa and 343 K

$W_1(-)$	$W_2(-)$	$W_3(-)$
	PMMA-15 k	
0.542	$4.26 \cdot 10^{-2}$	0.415
0.553	$2.43 \cdot 10^{-2}$	0.423
0.577	$1.05 \cdot 10^{-2}$	0.412
0.611	$4.16 \cdot 10^{-3}$	0.385
	PMMA-120 k	
0.466	$2.64 \cdot 10^{-2}$	0.507
0.504	$1.28 \cdot 10^{-2}$	0.483
0.528	$5.14 \cdot 10^{-3}$	0.467
0.540	$2.62 \cdot 10^{-3}$	0.458

point compositions of the CO_2 + PMMA + ethanol systems at 15 MPa and 343.2 K are shown in Figure 3 and Table 3. The solubility of PMMA decreases with an increase in the CO_2 concentration because CO_2 is a nonsolvent for PMMA, and ethanol is a relatively good solvent for PMMA at 343.2 K. The size of the two-phase region of PMMA-120 k is wider than that of PMMA-15k. This type of liquid–liquid phase behavior can be explained by the free volume of the polymer solution. The free volume of a polymer, which corresponds to the unoccupied regions accessible to segmental motions, strongly affects the phase behavior and molecular interaction of the polymer solution. The difference between the free volumes of the solvent and polymer causes the broadening observed in the liquid–liquid phase split area. The free volume generally decreases as the molecular size increases, and the polymer free volume is generally less than the solvent free volume.[20] It becomes increasingly more difficult to dissolve higher molecular weights of PMMA in the mixture of CO_2 and ethanol because the difference between the free volumes of the polymer and solvent increases with the polymer molecular weight.

Conclusion

To obtain further information about a polymer material formation technique that uses CO_2-expanded ethanol solution, the phase behavior of mixtures containing CO_2 and PMMA with different molecular weights (PMMA-15 k, PMMA-120 k) were examined. It has been observed that with the increase in the amount of CO_2 in the PMMA + ethanol solutions the UCST line shifts toward higher temperatures and pressures and the L−LV boundary shifts toward higher pressure. The addition of supercritical CO_2 into the polymer solutions makes the phase behaviors dependent on pressure.

Literature Cited

(1) Eckert, C. A.; Bush, D.; Brown, J. S.; Liotta, C. L. Tuning solvents for sustainable technology. *Ind. Eng. Chem. Res.* **2000**, *39* (12), 4615–4621.
(2) Eckert, C. A.; Liotta, C. L.; Bush, D.; Brown, J. S.; Hallett, J. P. Sustainable reactions in tunable solvents. *J. Phys. Chem. B* **2004**, *108* (47), 18108–18118.
(3) Anand, M.; McLeod, M. C.; Bell, P. W.; Roberts, C. B. Tunable solvation effects on the size-selective fractionation of metal nanoparticles in CO_2 gas-expanded solvents. *J. Phys. Chem. B* **2005**, *109* (48), 22852–22859.
(4) Xu, D. W.; Carbonell, R. G.; Kiserow, D. J.; Roberts, G. W. Hydrogenation of polystyrene in CO_2-expanded solvents: Catalyst poisoning. *Ind. Eng. Chem. Res.* **2005**, *44* (16), 6164–6170.
(5) Eckert, C.; Liotta, C.; Ragauskas, A.; Hallett, J.; Kitchens, C.; Hill, E.; Draucker, L. Tunable solvents for fine chemicals from the biorefinery. *Green Chem.* **2007**, *9* (6), 545–548.
(6) Donohue, M. D.; Geiger, J. L.; Kiamos, A. A.; Nielsen, K. A. *Green Chemistry: Designing. Chemistry for the Environment*; Anastas, P. T., Williamson, T. C., Eds.; American Chemical Society: Washington, DC, 1996; pp 152–167.
(7) Behme, S.; Sadowski, G.; Arlt, W. Modeling of the separation of polydisperse polymer systems by compressed gases. *Fluid Phase Equilib.* **1999**, *158−160*, 869–877.
(8) Coen, E. M.; Quinn, J. F.; Dehghani, F.; Foster, N. R.; Davis, T. P. Molecular weight fractionation of poly(methyl methacrylate) using Gas Anti-Solvent techniques. *Polymer* **2003**, *44* (12), 3477–3481.
(9) Matsuyama, K.; Mishima, K. Coacervation microencapsulation of talc particles with poly(methyl methacrylate) by pressure-induced phase separation of CO_2-expanded ethanol solutions. *Ind. Eng. Chem. Res.* **2007**, *46* (19), 6244–6250.
(10) Kirby, C. F.; McHugh, M. A. Phase behavior of polymers in supercritical fluid solvents. *Chem. Rev.* **1999**, *99* (2), 565–602.
(11) Kiamos, A. A.; Donohue, M. D. The effect of supercritical carbon dioxide on polymer-solvent mixtures. *Macromolecules* **1994**, *27* (2), 357–64.
(12) Kim, S.; Kim, Y. S.; Lee, S. B. Phase behaviors and fractionation of polymer solutions in supercritical carbon dioxide. *J. Supercrit. Fluids* **1998**, *13* (1–3), 99–106.
(13) Lee, J. M.; Lee, B. C.; Hwang, S. J. Phase behavior of Poly(L-lactide) in supercritical mixtures of carbon dioxide and chlorodifluoromethane. *J. Chem. Eng. Data* **2000**, *45* (6), 1162–1166.
(14) Joung, S. N.; Park, J. U.; Kim, S. Y.; Yoo, K. P. High-pressure phase behavior of polymer-solvent systems with addition of supercritical CO_2 at temperatures from 323.15 to 503.15 K. *J. Chem. Eng. Data* **2002**, *47* (2), 270–273.
(15) Sadowski, G. *Supercritical Carbon Dioxide in Polymer Reaction Engineering*; Kemmere, M. F., Meyer, T., Eds.; Wiley-VCH Verlag GmbH & Co.: Weinheim, 2005; pp15–35.
(16) Matsuyama, K.; Mishima, K. Phase behavior of CO_2 + polyethylene glycol +ethanol at pressures up to 20 MPa. *Fluid Phase Equilib.* **2006**, *249* (1–2), 173–178.
(17) Byun, H. S.; McHugh, M. A. Impact of "free" monomer concentration on the phase behavior of supercritical carbon dioxide-polymer mixtures. *Ind. Eng. Chem. Res.* **2000**, *39* (12), 4658–4662.
(18) Matsuyama, H.; Takida, Y.; Maki, T.; Teramoto, M. Preparation of porous membrane by combined use of thermally induced phase separation and immersion precipitation. *Polymer* **2002**, *43* (19), 5243–5248.
(19) Zeman, L.; Patterson, D. Pressure effects in polymer solution phase equilibriums. II. Systems showing upper and low critical solution temperatures. *J. Phys. Chem.* **1972**, *76* (8), 1214–1219.
(20) Chen, S. J.; Radosz, M. Density-tuned polyolefin phase equilibria. 1. Binary solutions of alternating poly(ethylene-propylene) in subcritical and supercritical propylene, 1-butene, and 1-hexene. Experiment and Flory-Patterson model. *Macromolecules* **1992**, *25* (12), 3089–3096.

Received for review December 18, 2007. Accepted February 21, 2008. This study was partially supported by a Grant-in-Aid for Young Scientists (19760537).

JE7007473